Bräutigam Konstantin (Orcid ID: 0000-0002-3966-3579)
Schürch Christian M. (Orcid ID: 0000-0002-1792-1768)

Comprehensive analysis of SARS-CoV-2 receptor proteins in human respiratory tissues identifies alveolar macrophages as potential virus entry site

Running title: SARS-CoV-2 entry proteins in alveolar macrophages

Konstantin Bräutigam[1], Stefan Reinhard[1], Martin Wartenberg[1], Stefan Forster[2], Karen Greif[3], Massimo Granai[3], Hans Bösmüller[3], Karin Klingel[3], Christian M. Schürch[3]*

[1]Institute of Pathology, University of Bern, 3008 Bern, Switzerland

[2]Department for BioMedical Research, University of Bern, 3010 Bern, Switzerland

[3]Department of Pathology and Neuropathology, University Hospital and Comprehensive Cancer Center Tübingen, Tübingen, Germany

*Corresponding author:

Christian M. Schürch

Department of Pathology and Neuropathology

Liebermeisterstr. 8, 72076 Tübingen, Germany

Email: christian.schuerch@med.uni-tuebingen.de

Number of tables: 3

Number of figures: 4

Word count: 3713

Keywords: SARS-CoV-2; COVID-19; receptor; macrophage; lectin

This article has been accepted for publication and undergone full peer review but has not been through the copyediting, typesetting, pagination and proofreading process which may lead to differences between this version and the Version of Record. Please cite this article as doi: 10.1111/his.14871

Abstract

Aims

COVID-19 has had enormous consequences on global health care and resulted in millions of fatalities. The exact mechanism and site of SARS-CoV-2 entry into the body remains insufficiently understood. Recently, novel virus receptors were identified, and alveolar macrophages were suggested as a potential viral entry cell type and vector for intra-alveolar virus transmission. Here, we investigated the protein expression of ten well-known and novel virus entry molecules along potential entry sites in humans using immunohistochemistry.

Methods and results

Samples of different anatomic sites from up to 93 patients were incorporated into tissue microarrays. Protein expression of ACE2, TMPRSS2, furin, CD147, C-type lectin receptors (CD169, CD209, CD299), neuropilin-1, ASGR1 and KREMEN1 were analyzed. In lung tissues, at least one of the three receptors ACE2, ASGR1 or KREMEN1 was expressed in the majority of cases. Moreover, all of the investigated molecules were found to be expressed in alveolar macrophages, and colocalization with SARS-CoV-2 N-protein was demonstrated using dual immunohistochemistry in lung tissue from a COVID-19 autopsy. While CD169 and CD209 showed consistent protein expression in sinonasal, conjunctival and bronchiolar tissues, neuropilin-1 and ASGR1 were mostly absent, suggesting a minor relevance of these two molecules at these specific sites.

Conclusion

Our results extend recent discoveries indicating a role for these molecules in virus entry at different anatomic sites. Moreover, they support the notion of alveolar macrophages being a potential entry cell for SARS-CoV-2.

Introduction

SARS-CoV-2 and its associated syndrome COVID-19 have taken a toll on humanity. Despite global vaccination campaigns and protective measures, viral transmission is not under control with infections on the rise.

Although intensely explored, the mechanism of SARS-CoV-2 viral entry is still insufficiently understood. Angiotensin-converting enzyme 2 (ACE2) with its main co-receptor Transmembrane protease serine 2 (TMPRSS2) (1) is widely regarded as the principal entry receptor (2). In the first months of the pandemic, furin and CD147 (basigin) have emerged as potential viral entry facilitators (1,3,4). Whereas the significance of furin--by cleaving the SARS-CoV-2 spike protein--in viral entry was scientifically proven (5), the importance of CD147 remains controversial (6,7).

Recently, several alternative viral entry molecules have been discovered. Three C-type lectin receptors, CD169 (Siglec-1, Sialoadhesin), CD209 (DC-SIGN) and CD299 (LSIGN, DC-SIGNR, C-type lectin domain family 4 member M [CLEC4M]), enhance ACE2-dependent viral entry in their role as attachment receptors (8–12). CD169 is a surface molecule expressed in macrophages of several anatomic sites that primarily promotes adhesion to neutrophils, and has been described as an entry mediator for retroviruses (13). CD209, mainly expressed on dendritic cells, and its receptor CD299 are known for their capability of viral capture and transmission of HIV and hepatitis C virus (14,15). Interestingly, CD209 expression was shown to facilitate viral transmission of SARS-CoV-1 from alveolar macrophages (AMs) to type II pneumocytes, inducing airway stress and dysfunction (16–18). Moreover, CD209 has been proposed to act as a SARS-CoV-2 receptor on liver sinusoidal endothelial cells (19). In addition, lectin proteins were shown to activate the complement system (20) and stir further inflammatory response by initiating cytokine production in

myeloid cells (21), which fits well into the established concept of inflammasome activation by SARS-CoV-2 (22).

Furthermore, Neuropilin-1 (NRP-1), originally described as a pro-angiogenic protein and a mediator for neuronal cell guidance in the developing nervous system (23), has been shown to potentiate viral transmission of SARS-CoV-2 (24–26). In addition, using genomic receptor profiling, the roles of Kringle Containing Transmembrane Protein 1 (KREMEN1) and asialoglycoprotein receptor 1 (ASGR1) as "receptor-like host factors" in SARS-CoV-2 have recently been proposed (27,28). Both proteins are described to act independently from ACE2. While KREMEN1 is a known entry receptor for multiple enteroviruses, such as coxsackievirus A10 (29,30), ASGR1, a C-type lectin receptor primarily expressed in hepatocytes (31), facilitates the entry of hepatitis B virus (32). Importantly, the expression and distribution of these novel SARS-CoV-2 viral entry molecules (CD169, CD209, CD299, NRP-1, ASGR1 and KREMEN1) along potential entry sites in humans has not been studied in detail so far.

Synchronously to the discovery of alternative viral entry molecules, monocytes and (alveolar) macrophages have been described as a potential vector cell for SARS-CoV-2 entry and transmission (33–38). Viral replication in AMs as well as viral uptake was demonstrated in mouse models (33,37) and using transcriptomic profiling (36). A cellular shift towards pro-inflammatory monocytes has been described in the alveoli (39). SARS-CoV-2 uses the M1 macrophage, with its distinct pro-inflammatory cytokine profile (40), as a vehicle for transmission and infection of the alveolar epithelium (33). In parallel, the ingestion of SARS-CoV-2 in monocytes elicits a strong inflammatory response (41,42), which is critical in COVID-19.

Here, we extend our previous work (43) by analyzing the (co)expression of ten potential viral entry molecules, ACE2, TMPRSS2, furin, CD147, CD169, CD209, CD299, NRP-1, ASGR1, KREMEN1, and address their clinical relevance and anatomic distribution. Moreover, expression patterns in AMs are delineated. Using dual immunohistochemistry on autopsy lung tissue from a patient who died of COVID-19, we demonstrate that SARS-CoV-2 N-protein is detectable in AMs expressing ACE2 and other entry receptors. Our work indicates an important role for AMs as a cellular hub for entry and transmission of SARS-CoV-2.

Methods

Patient samples

The patient samples include 95 sinonasal, 84 conjunctival, and 93 lung specimens. The most frequent diagnoses were sinusitis/nasal polyp (89/95; 93.7%), conjunctival pterygium (50/84; 59.5%), and cancer in the lung (48/93; 51.6%), respectively. Sinusitis/nasal polyp qualified as inflammatory. In non-cancerous lung samples, 19 (20.4%) showed emphysematous changes, and 7 (7.5%) an inflammatory condition, including bacterial pneumonia, aspergillosis, usual interstitial pneumonia, and hypersensitivity pneumonitis. In conjunctival specimens, 24 (28.6%) samples were operated due to tumorous conditions, e.g., nevi, cysts, and fibroepithelial polyps, and 7 (8.3%) had an inflammation. Further details are listed in **Table S1**. Tissues from three autopsies were included: SARS-CoV-2-infected lung tissue from a 84 year old female who died of COVID-19 pneumonia, and SARS-CoV-2-negative lung tissues from a 62 year old male with fungal pneumonia, as well as a 15 year old male with CMV pneumonia.

Briefly, tissue microarrays (TMAs) of formalin-fixed, paraffin-embedded conjunctival, sinonasal, bronchiolar and alveolar samples were used to determine receptor protein expression by immunohistochemistry. Data for ACE2, TMPRSS2, furin and CD147 are from our previous publication (43). The study was approved by the local ethics committee of the Canton of Bern, Switzerland (KEK 200/2014).

Immunohistochemistry (IHC)

For each specimen, three representative tissue cores of 0.6 mm diameter were assembled into TMAs using a Grand Master automated tissue microarrayer (3DHistech, Budapest, Hungary). 2.5 µm sections were deparaffinized in dewax solution (Leica Biosystems, Wetzlar,

Germany), and rehydrated. Single-stain IHCs were performed on a BOND RX automated immunostainer (Leica).

Primary antibodies were incubated for 30 min at room temperature and used as indicated in **Table S2**. Antibody detection was performed with the BOND Polymer Refine Detection kit (DS9800, Leica) using 3,3-diaminobenzidine (DAB) as a brown chromogen. The samples were counterstained with hematoxylin, dehydrated and mounted with Pertex (Sakura, Alphen aan den Rijn, Netherlands). Slides were scanned on a Pannoramic 250 Flash scanner (3DHistech). Dual-stain IHCs were performed on a Benchmark Ultra Immunostainer using the OptiView DAB detection kit for macrophage and receptor antibodies, and the UltraView Universal AP Red detection kit (Roche Diagnostics, Rotkreuz, Switzerland) for the SARS-CoV-2 N-protein antibody. Antibodies were incubated for 32 min at 37°C and used as indicated in **Table S2.** The anti-SARS-CoV-2 N-protein antibody has been described previously (44). Dual-stain IHC slides were photographed using a DS-Fi3 camera on an Eclipse Ni microscope with a 40x plan apochromat lambda objective, and NIS software (Nikon, Tokyo, Japan).

Placental, testicular, prostatic and renal tissues were used as positive and negative controls, respectively (**Figure S1**). Lung tissues from two non-COVID-19 autopsies (see patient samples) were used as SARS-CoV-2 negative controls.

TMA interpretation and statistics

TMA cores were evaluated in a blinded, independent and randomized manner by three pathologists (K.B., M.W., S.F.) using Scorenado, a web-based analysis tool (https://github.com/digitalpathologybern/scorenado) (45,46). Staining intensities for epithelium and stroma were quantified three-tiered: 0, negative; 1, low; and 2, moderate-strong. AMs were quantified four-tiered: 0, negative; 1, low; 2, moderate; 3, strong. Median

values across all observers were used for final analyses with decimal numbers rounded up. Scores were only included if tissue quality was deemed sufficient by at least two pathologists. Discrepant cases, i.e., a deviation of ≥ 1 in scoring, were jointly reviewed for a final consensus score. For consensus, at least two of three raters had to agree on the final score. The number of AMs was counted by eyeballing and arbitrarily quantified in a three-tiered manner for each tissue core: <10 AMs per core, low; 11 to 30 AMs per core, moderate; >30 AMs per core, high (**Figure S2**). Then, median values (up to three tissue cores per patient) were used for further analysis (details in **Table S3**). Maximum 71 conjunctival, 90 sinonasal, 81 bronchiolar, and 93 alveolar tissue samples were included for definite analysis. All samples were derived from biopsy or resection specimens of different patients (FFPE material from 2016 and before). In oncologic lung specimens, tissue cores were obtained from non-neoplastic lung parenchyma distant from the tumor region. Expression in stroma was jointly scored for immune cells and fibroblasts. In bronchioli, only epithelial expression was assessed.

Statistical analyses were performed using SPSS 28.0 (SPSS Inc., Chicago, USA). Two-sided Pearson chi-squared tests were used to calculate contingency tables. P-values <0.05 were considered statistically significant. Correlation analyses were conducted using Spearman-rho coefficients (ρ) in GraphpadPRISM 9 (GraphPad Software, Inc., San Diego, USA). Venn diagrams were drawn using the "VennDiagram" package (47) in R Studio (R Foundation for Statistical Computing, Vienna, Austria). Fleiss kappa (κ) was used to assess the strength of interobserver agreement for multiraters (48). Moreover, expression of molecules was compared in three arbitrarily defined age subgroups (0-30 yr; 31-60 yr; >60 yr).

Results

Consistent protein expression of CD169 and KREMEN1 in sinonasal, conjunctival and bronchiolar epithelium

The mucosal sites of the sinonasal tract and the conjunctiva are potential viral entry sites for SARS-CoV-2. We analyzed the expression of NRP-1, CD169, CD209, CD299, ASGR1 and KREMEN1 in up to 216 TMA cores of conjunctival, 270 cores of sinonasal and 243 cores of bronchiolar specimens, respectively. Initial interobserver agreement was "moderate" (global κ=0.530; 95% confidence interval [CI] 0.513-0.546; sinonasal specimens: κ=0.547; 95% CI 0.517-0.578; conjunctival specimens: κ=0.513; 95% CI 0.478-0.547; lung specimens: κ=0.509; 95% CI 0.483-0.534, further details in **Table S4**) before consensus was reached via discussion of discrepant scores.

We found that CD169 and KREMEN1 are expressed in sinonasal, conjunctival and bronchiolar epithelium in the majority of samples (**Table 1, Figure S3**). CD169 was expressed in 74/86 (86.0%) specimens of sinonasal epithelium, 54/71 (76.1%) specimens of conjunctival epithelium and 61/80 (76.3%) specimens of bronchiolar epithelium. KREMEN1 expression was found in the epithelium of 66/70 (94.3%) sinonasal, 58/60 (96.7%) conjunctival and 32/62 (51.6%) bronchiolar specimens. Stromal KREMEN1 expression was also detected in the majority of sinonasal specimens (48/70; 68.6%). At least one of the three receptors ACE2, ASGR1 or KREMEN1 was expressed in epithelial cells in 38/47 (80.1%) of the bronchiolar samples (**Figure 1A**), while CD209 was not expressed at all in bronchiolar epithelium (0/59; 0%, **Figure S3**). Strongest correlations of the investigated molecules were observed for CD169 in bronchiolar epithelium: CD169 expression significantly correlated with CD147 ($p<0.001$, ρ=0.544), furin ($p<0.001$, ρ=0.589), TMPRSS2 ($p<0.001$, ρ=0.519), NRP-1 ($p<0.001$, ρ=0.519) and ASGR1 ($p<0.001$, ρ=0.5) expression (**Table 2**).

In inflammatory conditions of the sinonasal tract, epithelial KREMEN1 expression was significantly lower (p=0.022), while epithelial CD169 expression was significantly higher (p=0.019) compared to non-inflammatory conditions. Inflamed conjunctival specimens demonstrated significantly higher (p<0.001) epithelial CD299 expression compared to non-inflammatory conditions. For the neoplastic samples of the conjunctiva, stromal CD299 expression was significantly higher (p=0.019) while epithelial KREMEN1 expression was lower (p=0.005) than in non-neoplastic conditions.

In summary, our data indicate that KREMEN1 and C-type lectin receptors, mainly CD169, are consistently expressed in three potential virus entry sites, and may be differentially regulated in inflammatory and neoplastic conditions, depending on receptor type and site of expression.

Strong protein expression of CD209 in sinonasal and conjunctival stroma

CD209 (DC-SIGN) is known as an entry receptor for SARS-CoV-1 and has been postulated as a candidate entry receptor for SARS-CoV-2 as well (10,16). In our study, we observed high CD209 expression in the stroma of both sinonasal (50/72; 69.4%) and conjunctival (45/48; 93.8%) samples (**Table 1, Figure S3**). CD299 (LSIGN or DC-SIGNR), the third lectin protein investigated, showed mostly absence of staining in sinonasal tissue, while its expression in conjunctival epithelium was detectable in the majority of cases with at least low-level expression in 37/66 (56.0%) specimens. NRP-1 and ASGR1 were not detected in sinonasal and conjunctival tissue in the majority of specimens (**Table 1**). No significant correlations of receptor expression with age, sex, history of malignancy, eosinophil count, allergy or the presence of fungi were found (**Figure S4**). Altogether, in the upper respiratory tract, we found a strong and reproducible stromal expression of CD209, a surface protein

specific for dendritic cells that has proven pathogen-binding capacity (14,15,49), with possible relevance for SARS-CoV-2 virus entry.

Expression of viral entry molecules in alveolar macrophages

The implication of AMs as viral entry cells, replication niche and infectious transmitters of SARS-CoV-2 has been recently described (33,36,37). We therefore analyzed the expression of seven potential receptor entry molecules, i.e., ACE2, NRP-1, CD169, CD209, CD299, ASGR1, KREMEN1, and their auxiliary molecules, TMPRSS2, furin and CD147, in AMs.

We found that all these molecules can be expressed in AMs, with heterogeneous strength of expression (**Table 3, Figure 2, Figure S5**). The highest protein expression levels were observed for furin and CD147, with at least moderate expression in 71/93 (76.3%) cases each. ACE2, CD209 and CD299 expression was low or absent in AMs in the majority of samples. NRP-1, ASGR1 and KREMEN1 showed low median expression levels. At least one of the three receptors ACE2, ASGR1 or KREMEN1 was expressed in 79/91 (86.9%) of the cases (**Figure 1B**). Interestingly, higher AM densities significantly correlated with higher expression levels for all molecules investigated (KREMEN1: $p=0.025$; all other markers $p<0.001$; **Figures S2 and S6**). While AM density was significantly higher ($p=0.016$) in normal alveolar tissue from lung specimens removed for a neoplasm compared to non-neoplastic specimens, a comparison between non-inflammatory and inflammatory lung conditions did not reveal any significant differences (data not shown).

Moreover, dual IHC revealed colocalization of SARS-CoV-2 N-protein with ACE2, TMPRSS2, ASGR1 and CD147 in SARS-CoV-2-positive autopsy lung tissue of an 84 year old female patient with lethal COVID-19 pneumonia. Interestingly, in this lung tissue CD209 expression was restricted to alveolar epithelium without being co-expressed in SARS-CoV-2 N-protein-positive AMs, and CD299 was completely negative (**Figure 3** and data not shown).

Except for KREMEN1, no expression of any of the investigated markers in the alveolar septae and pneumocytes was detected (**Figure S3**). While protein expression was positively correlated among all of the molecules (**Figure 4**), correlations with patient age, sex, concurrent malignancy or history of malignancy were not observed (**Figure S4**). A comparison between emphysematous and non-emphysematous samples did not reveal any significant expression differences in alveolar macrophages for any of the molecules. However, the expression of TMPRSS2 and CD169 in bronchiolar epithelium was significantly higher ($p=0.008$ and $p=0.042$, respectively) in emphysematous lung samples. On the other hand, furin ($p=0.005$), TMPRSS2 ($p=0.013$), and CD169 ($p=0.029$) expression was significantly higher in bronchiolar epithelium in a neoplastic context. In inflamed tissue, significantly lower CD169 ($p=0.014$) expression was observed in AMs; ASGR1 ($p=0.053$) and CD169 ($p=0.054$) only showed trends of lower expression in bronchiolar epithelium.

In summary, our data indicate that AMs are a potential cell type for viral entry, as they can express a relevant number of virus receptors and associated molecules capable of binding and capturing the virus, and show positive immunostaining for SARS-CoV-2 N-protein in COVID-19 infected lung tissue (33).

Discussion

We previously found that ACE2 is only weakly expressed in the lower human respiratory tract. Moreover, preliminary analysis of our data indicated that AMs consistently expressed ACE2, TMPRSS2, furin and CD147 (43). Here we extended our analyses by several additional molecules potentially relevant for viral entry of SARS-CoV-2 that have not been systematically investigated in the respiratory tract so far.

CD169 was shown to be expressed on circulating monocytes (50) and dendritic cells (51). This further highlights mononuclear phagocytes as important potential viral entry cells

(52,53). In addition, CD169 is a known viral entry receptor with pathogen recognition ability (54). Here, we observed consistent expression of CD169 in sinonasal, conjunctival and bronchiolar epithelium, which supports its suggested role as an attachment receptor for SARS-CoV-2 (12). Siglec(-9) agonists can inhibit neutrophils in COVID-19, underlining potential therapeutic implications as well (55). While CD209 is robustly expressed in conjunctival stroma, CD299, a homologue of CD209, was undetectable in the majority of sinonasal and conjunctival tissues and bronchiolar epithelial cells. CD209 is a proven receptor for SARS-CoV-1 (16), and the conjunctivae are not to be neglected as a potential virus entry site (56,57).

KREMEN1 and ASGR1 have been described as ACE2-independent receptors forming specific "ASK-receptor combinations" (ASK: ACE2/ASGR1/KREMEN1), which determine SARS-CoV-2 susceptibility (27). It is hypothesized that dual or triple positivity of these three receptors leads to higher susceptibility. While KREMEN1 was consistently, though weakly, expressed in the sinonasal, conjunctival and bronchiolar epithelium, ASGR1 expression was mostly undetectable in all the investigated anatomic locations in our study. According to single-cell RNA sequencing data, both proteins are expressed in epithelium and immune cells with a general predominance of KREMEN1-positive cells (27). The expression of one "ASK" receptor is described as sufficient for viral entry. Here, in bronchiolar epithelium, at least one of these three molecules was expressed in the majority of cases.

NRP-1 has been revealed as a SARS-CoV-2 host factor using cell lines (24,25). So far, the protein expression of NRP-1 in respiratory mucosa has been investigated in autopsy material of six patients with confirmed SARS-CoV-2 infection (25). In our study, NRP-1 was mostly absent or weakly expressed in healthy conjunctival, sinonasal and bronchiolar epithelium.

Interestingly, we found expression of all investigated molecules in AMs. Moreover, they showed significant and strong positive correlation among each other, suggesting diverse expression profiles (high and low-expressors) of these molecules. The strength of expression significantly correlated with a higher AM density as well. Recently, AMs have been described as the "Achilles heel" (58) of COVID-19 with an important role in viral entry and transmission (33), making them a potential virus target (35). In line with this, we detected SARS-CoV-2 N-protein in AMs. Surprisingly, in our study, the highest expression levels in AMs were observed for furin and CD147. Both proteins are no key entry receptors, but rather auxiliary entry molecules. CD147 has been described to be involved in platelet activation in COVID-19 (59). A mechanistic role in (alveolar) macrophages is currently unknown; however, treatment with anti-CD147 antibodies showed improved recovery in COVID-19 pneumonia (60). Among all molecules, ACE2 expression in AMs was lowest with absence of expression in the majority of cases. However, in the vast majority of patients at least one of the "ASK" receptor molecules was expressed in AMs, with "triple negativity" in 13.1% of samples only.

Our study has several limitations. First, despite allowing for simultaneous assessment of multiple tissues and overcoming batch effects in stainings, protein expression analysis in TMAs could lead to loss of information due to small amounts of tissue being analyzed. For example, in bronchioli, we only investigated epithelial expression, but not subepithelial compartments such as peribronchiolar stroma or smooth muscle. Moreover, initial interobserver agreement was poor for NRP-1, CD209, ASGR1, and KREMEN1 in the stromal tissue compartments, and for NRP-1, CD209, CD299 in bronchiolar epithelium (**Table S4**). This could have been due to the paucity of analyzable cells in the stroma, or the small TMA core size for epithelium assessment, respectively.

Second, SARS-CoV-2 mRNA has been detected in type II pneumocytes (61). Here, pneumocytes were negative for most entry receptors except for weak KREMEN1 expression. Although we did not differentiate between type II and the more abundant type I pneumocytes, and KREMEN1 might mediate viral entry in the absence of other receptors, it is possible that viral entry is mediated by receptors expressed below the detection limit of IHC. Third, using dual immunohistochemistry we detected SARS-CoV-2 N-protein in AMs expressing several entry receptors. However, this analysis was only performed on tissue from a single patient, which precluded the analysis of possible inter-individual variations in the co-expression of these receptors along SARS-CoV-2 N-protein in COVID-19-diseased lungs. Fourth, although tissue cores from oncologic lung specimens were taken distant from the tumor, a microenvironmental shift in non-neoplastic lung parenchyma of tumor-bearing samples could lead to altered biomarker expression. Additionally, smoking habits or comorbidities of the included patients were unknown. Cigarette smoking can alter receptor protein expression (62), and also influences the alveolar compartment's local immune state (63), e.g., by recruiting AMs (64). Concordantly, AM density was significantly higher in cancerous lungs, and TMPRSS2 and CD169 expression was significantly higher in bronchiolar epithelium of samples with emphysema, both smoking-associated conditions.

In summary, first, the mechanistic relevance of AMs in SARS-CoV-2 susceptibility and transmission is further substantiated by the herein observed protein expression of all investigated molecules and the colocalization with SARS-CoV-2 N-protein. Second, ACE2 seems, at least based on protein expression, not to be a single-handed player in the respiratory tract but rather part of an orchestrated entry complex. Third, C-type lectin proteins CD169 and CD209 showed consistent expression in all the investigated anatomic locations, though most often at low levels. The relevance of NRP-1 and CD299 in the respiratory tract is questionable due to absence of expression in most samples.

Acknowledgements

The authors acknowledge the Translational Research Unit at the Institute of Pathology, University of Bern, Switzerland, for excellent technical support, and Tissuebank Bern for providing human tissue samples.

Statement of Ethics

The TMA study was approved by the local ethics committee of the Canton of Bern, Switzerland (KEK 200/2014). Tissues from autopsies were obtained with informed consent from the next of kin, and their use was approved by the institutional review board of the University of Tübingen (224/2021BO2).

Conflict of Interest Statement

The authors have no conflicts of interest to declare.

Funding Sources

This work was supported by the SwissLife Jubiläumsstiftung and in part by special funds from the state of Baden-Württemberg for autopsy-based COVID-19 research and the DEFEAT PANDEMIcs network funded by the BMBF.

Author Contributions

K.B. and C.M.S. designed the study, analyzed and interpreted data, and wrote the manuscript. S.R. provided the scoring software and processed data. M.W. and S.F. analyzed data. K.G. performed immunohistochemistry stainings. M.G., H.B. and K.K. provided autopsy tissues and critical reagents, and analyzed data. All authors revised the manuscript and approved its final version.

Data Availability Statement

Raw data are available from the corresponding author upon reasonable request.

References

1. Bestle D, Heindl MR, Limburg H, Van Lam van T, Pilgram O, Moulton H, et al. TMPRSS2 and furin are both essential for proteolytic activation of SARS-CoV-2 in human airway cells. Life Sci Alliance. 2020 Sep 1;3(9):e202000786.
2. Hoffmann M, Kleine-Weber H, Schroeder S, Krüger N, Herrler T, Erichsen S, et al. SARS-CoV-2 Cell Entry Depends on ACE2 and TMPRSS2 and Is Blocked by a Clinically Proven Protease Inhibitor. Cell [Internet]. 2020 Mar 5 [cited 2020 Mar 27]; Available from: http://www.sciencedirect.com/science/article/pii/S0092867420302294
3. Johnson BA, Xie X, Bailey AL, Kalveram B, Lokugamage KG, Muruato A, et al. Loss of furin cleavage site attenuates SARS-CoV-2 pathogenesis. Nature. 2021 Mar 1;591(7849):293–9.
4. Liu C, von Brunn A, Zhu D. Cyclophilin A and CD147: novel therapeutic targets for the treatment of COVID-19. Med Drug Discov. 2020 Sep 1;7:100056.
5. Essalmani R, Jain J, Susan-Resiga D, Andréo U, Evagelidis A, Derbali RM, et al. Distinctive Roles of Furin and TMPRSS2 in SARS-CoV-2 Infectivity. J Virol. 2022 Mar 28;96(8):e00128-22.
6. Ragotte RJ, Pulido D, Donnellan FR, Gorini G, Davies H, Brun J, et al. Human basigin (CD147) does not directly interact with SARS-CoV-2 spike glycoprotein. bioRxiv. 2021 Jan 1;2021.02.22.432402.
7. Shilts J, Crozier TWM, Greenwood EJD, Lehner PJ, Wright GJ. No evidence for basigin/CD147 as a direct SARS-CoV-2 spike binding receptor. Sci Rep. 2021 Jan 11;11(1):413.
8. Rahimi N. C-type Lectin CD209L/L-SIGN and CD209/DC-SIGN: Cell Adhesion Molecules Turned to Pathogen Recognition Receptors. Biology. 2021;10(1).
9. Guo L, Liang Y, Li H, Zheng H, Yang Z, Chen Y, et al. Epigenetic glycosylation of SARS-CoV-2 impact viral infection through DC&L-SIGN receptors. iScience. 2021 Dezember;24(12):103426.
10. Amraei R, Yin W, Napoleon MA, Suder EL, Berrigan J, Zhao Q, et al. CD209L/L-SIGN and CD209/DC-SIGN Act as Receptors for SARS-CoV-2. ACS Cent Sci. 2021 Jul 28;7(7):1156–65.
11. Thépaut M, Luczkowiak J, Vivès C, Labiod N, Bally I, Lasala F, et al. DC/L-SIGN recognition of spike glycoprotein promotes SARS-CoV-2 trans-infection and can be inhibited by a glycomimetic antagonist. PLOS Pathog. 2021 May 20;17(5):e1009576.
12. Lempp FA, Soriaga LB, Montiel-Ruiz M, Benigni F, Noack J, Park YJ, et al. Lectins enhance SARS-CoV-2 infection and influence neutralizing antibodies. Nature. 2021 Oct;598(7880):342–7.
13. Sewald X, Ladinsky MS, Uchil PD, Beloor J, Pi R, Herrmann C, et al. Retroviruses use CD169-mediated trans-infection of permissive lymphocytes to establish infection. Science. 2015 Oct 30;350(6260):563–7.
14. Lozach PY, Amara A, Bartosch B, Virelizier JL, Arenzana-Seisdedos F, Cosset FL, et al. C-type Lectins L-SIGN and DC-SIGN Capture and Transmit Infectious Hepatitis C Virus Pseudotype Particles *. J Biol Chem. 2004 Jul 30;279(31):32035–45.
15. Geijtenbeek TBH, Kwon DS, Torensma R, Vliet SJ van, Duijnhoven GCF van, Middel J, et al. DC-SIGN, a Dendritic Cell–Specific HIV-1-Binding Protein that Enhances trans-Infection of T Cells. Cell. 2000 Mar 3;100(5):587–97.
16. Jeffers SA, Tusell SM, Gillim-Ross L, Hemmila EM, Achenbach JE, Babcock GJ, et al. CD209L (L-SIGN) is a receptor for severe acute respiratory syndrome coronavirus. Proc Natl Acad Sci. 2004 Nov 2;101(44):15748–53.
17. Marzi Andrea, Gramberg Thomas, Simmons Graham, Möller Peggy, Rennekamp Andrew J., Krumbiegel Mandy, et al. DC-SIGN and DC-SIGNR Interact with the Glycoprotein of Marburg Virus and the S Protein of Severe Acute Respiratory Syndrome Coronavirus. J Virol. 2004 Nov 1;78(21):12090–5.
18. Soilleux EJ, Morris LS, Leslie G, Chehimi J, Luo Q, Levroney E, et al. Constitutive and induced expression of DC-SIGN on dendritic cell and macrophage subpopulations in situ and in vitro. J Leukoc Biol. 2002 Mar;71(3):445–57.
19. Kondo Y, Larabee JL, Gao L, Shi H, Shao B, Hoover CM, et al. L-SIGN is a receptor on liver

sinusoidal endothelial cells for SARS-CoV-2 virus. JCI Insight [Internet]. 2021 Jul 22 [cited 2021 Dec 24];6(14). Available from: https://insight.jci.org/articles/view/148999
20. Ali YM, Ferrari M, Lynch NJ, Yaseen S, Dudler T, Gragerov S, et al. Lectin Pathway Mediates Complement Activation by SARS-CoV-2 Proteins. Front Immunol [Internet]. 2021 [cited 2022 Jan 17];12. Available from: https://www.frontiersin.org/article/10.3389/fimmu.2021.714511
21. Lu Q, Liu J, Zhao S, Castro MFG, Laurent-Rolle M, Dong J, et al. SARS-CoV-2 exacerbates proinflammatory responses in myeloid cells through C-type lectin receptors and Tweety family member 2. Immunity. 2021 Jun 8;54(6):1304-1319.e9.
22. Vora SM, Lieberman J, Wu H. Inflammasome activation at the crux of severe COVID-19. Nat Rev Immunol. 2021 Nov;21(11):694–703.
23. Soker S, Takashima S, Miao HQ, Neufeld G, Klagsbrun M. Neuropilin-1 Is Expressed by Endothelial and Tumor Cells as an Isoform-Specific Receptor for Vascular Endothelial Growth Factor. Cell. 1998 Mar 20;92(6):735–45.
24. Daly JL, Simonetti B, Klein K, Chen KE, Williamson MK, Antón-Plágaro C, et al. Neuropilin-1 is a host factor for SARS-CoV-2 infection. Science [Internet]. 2020 Nov 13 [cited 2022 Jan 21]; Available from: https://www.science.org/doi/abs/10.1126/science.abd3072
25. Cantuti-Castelvetri L, Ojha R, Pedro LD, Djannatian M, Franz J, Kuivanen S, et al. Neuropilin-1 facilitates SARS-CoV-2 cell entry and infectivity. Science [Internet]. 2020 Nov 13 [cited 2022 Jan 17]; Available from: https://www.science.org/doi/abs/10.1126/science.abd2985
26. Kyrou I, Randeva HS, Spandidos DA, Karteris E. Not only ACE2—the quest for additional host cell mediators of SARS-CoV-2 infection: Neuropilin-1 (NRP1) as a novel SARS-CoV-2 host cell entry mediator implicated in COVID-19. Signal Transduct Target Ther. 2021 Jan 18;6(1):1–3.
27. Gu Y, Cao J, Zhang X, Gao H, Wang Y, Wang J, et al. Receptome profiling identifies KREMEN1 and ASGR1 as alternative functional receptors of SARS-CoV-2. Cell Res. 2022 Jan;32(1):24–37.
28. Hoffmann M, Pöhlmann S. Novel SARS-CoV-2 receptors: ASGR1 and KREMEN1. Cell Res. 2022 Jan;32(1):1–2.
29. Staring J, Hengel LG van den, Raaben M, Blomen VA, Carette JE, Brummelkamp TR. KREMEN1 Is a Host Entry Receptor for a Major Group of Enteroviruses. Cell Host Microbe. 2018 May 9;23(5):636-643.e5.
30. Zhao Y, Zhou D, Ni T, Karia D, Kotecha A, Wang X, et al. Hand-foot-and-mouth disease virus receptor KREMEN1 binds the canyon of Coxsackie Virus A10. Nat Commun. 2020 Jan 7;11(1):38.
31. Hoober JK. ASGR1 and Its Enigmatic Relative, CLEC10A. Int J Mol Sci. 2020 Jan;21(14):4818.
32. Zhang X, Lin S mei, Chen T yan, Liu M, Ye F, Chen Y ru, et al. Asialoglycoprotein receptor interacts with the preS1 domain of hepatitis B virus in vivo and in vitro. Arch Virol. 2011 Apr 1;156(4):637–45.
33. Lv J, Wang Z, Qu Y, Zhu H, Zhu Q, Tong W, et al. Distinct uptake, amplification, and release of SARS-CoV-2 by M1 and M2 alveolar macrophages. Cell Discov. 2021 Apr 13;7(1):1–12.
34. Abassi Z, Knaney Y, Karram T, Heyman SN. The Lung Macrophage in SARS-CoV-2 Infection: A Friend or a Foe? Front Immunol [Internet]. 2020 [cited 2021 May 22];11. Available from: http://www.frontiersin.org/articles/10.3389/fimmu.2020.01312/full
35. Gracia-Hernandez M, Sotomayor EM, Villagra A. Targeting Macrophages as a Therapeutic Option in Coronavirus Disease 2019. Front Pharmacol. 2020;11:1659.
36. Grant RA, Morales-Nebreda L, Markov NS, Swaminathan S, Querrey M, Guzman ER, et al. Circuits between infected macrophages and T cells in SARS-CoV-2 pneumonia. Nature. 2021 Feb;590(7847):635–41.
37. Sefik E, Qu R, Junqueira C, Kaffe E, Mirza H, Zhao J, et al. Inflammasome activation in infected macrophages drives COVID-19 pathology. Nature. 2022 Jun;606(7914):585–93.
38. Bost P, Giladi A, Liu Y, Bendjelal Y, Xu G, David E, et al. Host-Viral Infection Maps Reveal Signatures of Severe COVID-19 Patients. Cell. 2020 Jun 25;181(7):1475-1488.e12.
39. Chen ST, Park MD, Valle DMD, Buckup M, Tabachnikova A, Simons NW, et al. Shift of lung macrophage composition is associated with COVID-19 disease severity and recovery [Internet]. bioRxiv; 2022 [cited 2022 Aug 1]. p. 2022.01.11.475918. Available from: https://www.biorxiv.org/content/10.1101/2022.01.11.475918v1

40. Sica A, Mantovani A. Macrophage plasticity and polarization: in vivo veritas. J Clin Invest. 2012 Mar 1;122(3):787–95.
41. Junqueira C, Crespo Â, Ranjbar S, de Lacerda LB, Lewandrowski M, Ingber J, et al. FcγR-mediated SARS-CoV-2 infection of monocytes activates inflammation. Nature. 2022 Apr 6;1–13.
42. Merad M, Martin JC. Pathological inflammation in patients with COVID-19: a key role for monocytes and macrophages. Nat Rev Immunol. 2020 Jun;20(6):355–62.
43. Bräutigam K, Reinhard S, Galván JA, Wartenberg M, Hewer E, Schürch CM. Systematic Investigation of SARS-CoV-2 Receptor Protein Distribution along Viral Entry Routes in Humans. Respiration [Internet]. 2022; Available from: https://www.karger.com/DOI/10.1159/000521317
44. Disse SC, Manuylova T, Adam K, Lechler A, Zant R, Klingel K, et al. COVID-19 in 28-Week Triplets Caused by Intrauterine Transmission of SARS-CoV-2—Case Report. Front Pediatr [Internet]. 2021 [cited 2022 Oct 22];9. Available from: https://www.frontiersin.org/articles/10.3389/fped.2021.812057
45. Lytle NK, Ferguson LP, Rajbhandari N, Gilroy K, Fox RG, Deshpande A, et al. A Multiscale Map of the Stem Cell State in Pancreatic Adenocarcinoma. Cell. 2019/04/04 ed. 2019 Apr 18;177(3):572-586.e22.
46. 14(th) European Congress on Digital Pathology. J Pathol Inform. 2019 Nov 11;10:32.
47. Chen H, Boutros PC. VennDiagram: a package for the generation of highly-customizable Venn and Euler diagrams in R. BMC Bioinformatics. 2011 Jan 26;12(1):35.
48. Landis JR, Koch GG. The Measurement of Observer Agreement for Categorical Data. Biometrics. 1977;33(1):159–74.
49. Granelli-Piperno A, Pritsker A, Pack M, Shimeliovich I, Arrighi JF, Park CG, et al. Dendritic Cell-Specific Intercellular Adhesion Molecule 3-Grabbing Nonintegrin/CD209 Is Abundant on Macrophages in the Normal Human Lymph Node and Is Not Required for Dendritic Cell Stimulation of the Mixed Leukocyte Reaction. J Immunol. 2005 Oct 1;175(7):4265–73.
50. Doehn JM, Tabeling C, Biesen R, Saccomanno J, Madlung E, Pappe E, et al. CD169/SIGLEC1 is expressed on circulating monocytes in COVID-19 and expression levels are associated with disease severity. Infection. 2021 Aug 1;49(4):757–62.
51. Perez-Zsolt D, Muñoz-Basagoiti J, Rodon J, Elosua-Bayes M, Raïch-Regué D, Risco C, et al. SARS-CoV-2 interaction with Siglec-1 mediates trans-infection by dendritic cells. Cell Mol Immunol. 2021 Dec;18(12):2676–8.
52. Brufsky A, Lotze MT. DC/L-SIGNs of hope in the COVID-19 pandemic. J Med Virol. 2020;92(9):1396–8.
53. Jalloh S, Olejnik J, Berrigan J, Nisa A, Suder EL, Akiyama H, et al. CD169-mediated restrictive SARS-CoV-2 infection of macrophages induces pro-inflammatory responses. PLOS Pathog. 2022 Oct 24;18(10):e1010479.
54. Crocker PR, Paulson JC, Varki A. Siglecs and their roles in the immune system. Nat Rev Immunol. 2007 Apr;7(4):255–66.
55. Delaveris C, Wilk A, Riley N, Stark J, Yang S, Rogers A, et al. Synthetic Siglec-9 Agonists Inhibit Neutrophil Activation Associated with COVID-19. 2020 Dec 17 [cited 2021 Dec 23]; Available from: https://chemrxiv.org/engage/chemrxiv/article-details/60c75305469df463f7f44ca1
56. Hui KPY, Cheung MC, Perera RAPM, Ng KC, Bui CHT, Ho JCW, et al. Tropism, replication competence, and innate immune responses of the coronavirus SARS-CoV-2 in human respiratory tract and conjunctiva: an analysis in ex-vivo and in-vitro cultures. Lancet Respir Med. 2020 Jul 1;8(7):687–95.
57. Jackson RM, Hatton CF, Spegarova JS, Georgiou M, Collin J, Stephenson E, et al. Conjunctival epithelial cells resist productive SARS-CoV-2 infection. Stem Cell Rep. 2022 Jul 12;17(7):1699–713.
58. Wang Z, Li S, Huang B. Alveolar macrophages: Achilles' heel of SARS-CoV-2 infection. Signal Transduct Target Ther. 2022 Jul 19;7(1):1–9.
59. Maugeri N, De Lorenzo R, Clementi N, Antonia Diotti R, Criscuolo E, Godino C, et al. Unconventional CD147-dependent platelet activation elicited by SARS-CoV-2 in COVID-19. J Thromb Haemost. 2022;20(2):434–48.
60. Bian H, Zheng ZH, Wei D, Zhang Z, Kang WZ, Hao CQ, et al. Meplazumab treats COVID-19

pneumonia: an open-labelled, concurrent controlled add-on clinical trial [Internet]. medRxiv; 2020 [cited 2022 Dec 1]. p. 2020.03.21.20040691. Available from: https://www.medrxiv.org/content/10.1101/2020.03.21.20040691v3
61. Acheampong KK, Schaff DL, Emert BL, Lake J, Reffsin S, Shea EK, et al. Subcellular Detection of SARS-CoV-2 RNA in Human Tissue Reveals Distinct Localization in Alveolar Type 2 Pneumocytes and Alveolar Macrophages. mBio. 2022 Feb 8;13(1):e03751-21.
62. Matusiak M, Schürch CM. Expression of SARS-CoV-2 entry receptors in the respiratory tract of healthy individuals, smokers and asthmatics. Respir Res. 2020 Dec;21(1):252.
63. Pribul PK, Harker J, Wang B, Wang H, Tregoning JS, Schwarze J, et al. Alveolar Macrophages Are a Major Determinant of Early Responses to Viral Lung Infection but Do Not Influence Subsequent Disease Development. J Virol. 2008 May;82(9):4441–8.
64. Wallace WA, Gillooly M, Lamb D. Intra-alveolar macrophage numbers in current smokers and non-smokers: a morphometric study of tissue sections. Thorax. 1992 Jun;47(6):437.
65. Schober P, Boer C, Schwarte LA. Correlation Coefficients: Appropriate Use and Interpretation. Anesth Analg. 2018 May;126(5):1763–8.

Figure legends

Figure 1. ACE2/ASGR1/KREMEN1 receptor combinations in human lung tissue. Venn diagrams demonstrating combined expression of ACE2/ASGR1/KREMEN1 ("ASK" receptors (27)) in bronchiolar epithelium (**A**, n=47) and alveolar macrophages (AMs) (**B**, n=91). No expression of any of the molecules ("triple negative") in bronchiolar epithelium of nine patients (9/47, 19.1%), and in AMs of twelve patients (12/91, 13.2%). Expression of all three molecules in AMs of 30/91 (33.0%) patients. Green, ACE2+; orange, KREMEN1+; blue, ASGR1+; pink, triple negative.

Figure 2. Expression of NRP-1, CD169, CD209, CD299, ASGR1 and KREMEN1 in alveolar macrophages. Representative IHC images out of 279 TMA cores, **A:** no expression, **B:** strong expression (extended version in **Figure S5**). Scale bar, 200 µm; inset, 20 µm.

Figure 3. Co-expression of SARS-CoV-2 N-protein and ACE2, TMPRSS2, ASGR1 and CD163 in SARS-CoV-2 infected lung tissue. Representative dual IHC images demonstrating co-expression in AMs in autopsy-derived FFPE lung tissue from an 84 year old female patient who died of COVID-19 pneumonia with acute respiratory distress syndrome. SARS-CoV-2 N-protein, red chromogen; ACE2/TMPRSS2/ASGR1/CD163, brown chromogen, respectively. Scale bar, 20 µm.

Figure 4. Correlation matrix for alveolar macrophages. Non-Gaussian Spearman's ρ correlation matrix (heat map) reveals significant (independent values, n=92, two-tailed $p < 0.0001$) positive correlation among all molecules in AMs.

Figure S1. Staining controls. Low (+) NRP-1 expression in proximal tubules of the kidney **(A)**. Absence of expression in testicular (-) **(B)**, prostatic (-) **(C)** and placental (-) **(D)** parenchyma. Low to moderate (+/++) CD169 expression in proximal tubules of the kidney **(E)**. Absence of CD169 expression in testicular (-) **(F)**, prostatic (-) **(G)** and placental (-) **(H)** parenchyma. Absence of CD209 expression in renal (-) **(I)**, testicular (-) **(J)** and prostatic (-) **(K)** parenchyma. CD209 expression in placental Hofbauer cells (++) **(L)**. Absence of CD299 expression in renal (-) **(M)**, testicular (-) **(N)**, prostatic (-) **(O)** and placental (-) **(P)** parenchyma. ASGR1 positivity in corpora amylacea of the prostate (+) **(S)**. Absence of ASGR1 expression in renal (-) **(Q)**, testicular (-) **(R)** and placental (-) **(T)** parenchyma. Absence of KREMEN1 expression in renal (-) **(U)**, testicular (-) **(V)** and placental (-) **(X)** parenchyma. KREMEN1 expression in prostatic acinar epithelium (+) **(W)**. Scale bar, 200 µm; inset, 20 µm.

Figure S2. Alveolar macrophage (AM) density. Representative IHC images (NRP-1) demonstrating the three-tiered quantification of AM density in tissue cores of alveolar lung parenchyma. The strength of expression correlates with the number of AMs. Scale bar, 200 µm; inset, 50 µm.

Figure S3. Representative stainings of epithelial and stromal expression for the investigated molecules. (A-C) NRP-1 expression (n=239 TMA cores) in **(A)** sinonasal, **(B)** bronchial, and **(C)** conjunctival specimens. **(D-F)** CD169 expression (n=242 TMA cores) in **(D)** sinonasal, **(E)** bronchial, and **(F)** conjunctival specimens. **(G-I)** CD209 expression (n=179 TMA cores) in **(G)** sinonasal, **(H)** bronchial, and **(I)** conjunctival specimens. **(J-L)** CD299 expression (n=240 TMA cores) in **(J)** sinonasal, **(K)** bronchial, and **(L)** conjunctival specimens. **(M-O)** ASGR1 expression (n=225 TMA cores) in **(M)** sinonasal, **(N)** bronchial,

and **(O)** conjunctival specimens. **(P-R)** KREMEN1 expression (n=192 TMA cores) in **(P)** sinonasal, **(Q)** bronchial, and **(R)** conjunctival specimens. Left panels, absence of expression; center panels, low expression (1), right panels, high expression (2), respectively (presence of expression in accordance with **Table 1**). Scale bar, 200 µm; inset, 20 µm.

Figure S4. Correlation matrices. Non-Gaussian Spearman's ρ correlation matrix (heat map) showing all correlations for each anatomic site (sinonasal tract, conjunctiva, bronchioli). Ticked boxes are excluded from analysis.

Figure S5. Expression of NRP-1, CD169, CD209, CD299, ASGR1 and KREMEN1 in alveolar macrophages. Representative IHC images out of 279 TMA cores. **(A)** No expression, **(B)** low expression (1), **(C)** moderate expression (2), **(D)** strong expression (3). Scale bar, 200 µm; inset, 20 µm.

Figure S6. Intensity of receptor molecule expression with respect to AM density.

Table 1 Expression of NRP-1, CD169, CD209, CD299, ASGR1 and KREMEN1 in epithelium (top row) and stroma (bottom row) of sinonasal tract, conjunctivae, and bronchioli, respectively. The following scores were applied: 0, no expression / negative; 1, low expression; 2, high expression.

Sinonasal tract		**Median**	**Mean**	**negative, n/n (%)**	**low, n/n (%)**	**high, n/n (%)**
NRP-1	epithelial stromal	0 0	0.5 0.1	45/86 (52.3) 80/89 (89.9)	36/86 (41.9) 8/89 (9.0)	5/86 (5.8) 1/89 (1.1)
CD169	epithelial stromal	1 0	1.2 0.4	12/86 (14.0) 67/90 (74.4)	49/86 (57.0) 14/90 (15.6)	25/86 (29.1) 9/90 (10.0)
CD209	epithelial stromal	0 2	0.2 1.7	56/67 (83.6) 3/72 (4.2)	11/67 (16.4) 19/72 (26.4)	0/67 50/72 (69.4)
CD299	epithelial stromal	0 0	0.2 0	70/87 (80.5) 89/90 (98.9)	17/87 (19.5) 1/90 (1.1)	0/87 (0) 0/90 (0)
ASGR1	epithelial stromal	0 0	0.4 0	57/85 (67.1) 84/86 (97.7)	19/85 (22.4) 2/86 (2.3)	9/85 (10.6) 0/86 (0)
KREMEN1	epithelial stromal	1 1	1.3 0.8	4/70 (5.7) 22/70 (31.4)	41/70 (58.6) 39/70 (55.7)	25/70 (35.7) 9/70 (12.9)
Conjunctivae						
NRP-1	epithelial stromal	0 0	0.3 0.1	51/68 (75.0) 65/69 (94.2)	17/68 (25.0) 4/69 (5.8)	0/68 0/69
CD169	epithelial stromal	1 0	0.8 0.1	17/71 (23.9) 67/72 (93.1)	51/71 (71.8) 5/72 (6.9)	3/71 (4.2) 0/72
CD209	epithelial stromal	0 2	0 1.9	53/53 (100) 0/48	0/53 3/48 (6.3)	0/53 45/48 (93.8)
CD299	epithelial stromal	1 0	0.6 0.1	29/66 (43.9) 68/70 (97.1)	35/66 (53.0) 0/70	2/66 (3.0) 2/70 (2.9)
ASGR1	epithelial stromal	0 0	0.1 0	61/65 (93.8) 64/64 (100)	4/65 (6.2) 0/64	0/65 0/64
KREMEN1	epithelial stromal	2 0	1.5 0.4	2/60 (3.3) 31/52 (59.6)	26/60 (43.3) 20/52 (38.5)	32/60 (53.3) 1/52 (1.9)
Bronchioli						
NRP-1	epithelial	0	0.5	42/81 (51.9)	38/81 (46.9)	1/81 (1.2)
CD169	epithelial	1	1.1	19/80 (23.8)	38/80 (47.5)	23/80 (28.7)
CD209	epithelial	0	0	59/59 (100)	0/59	0/59

CD299	epithelial	0	0.1	73/80 (91.3)	7/80 (8.8)	0/80
ASGR1	epithelial	0	0.7	39/74 (52.7)	21/74 (28.4)	14/74 (18.9)
KREMEN1	epithelial	1	0.7	30/62 (48.4)	20/62 (32.3)	12/62 (19.4)

Table 2 Correlation table showing significant correlation coefficients ($p<0.05$), for correlations with at least moderate strength (Spearman's $\rho > 0.4$ (65)) in sinonasal, conjunctival and bronchiolar specimens (all correlations in **Figure S4**). Columns represent epithelial expression (unless otherwise specified as stromal) for each molecule in its corresponding anatomic site.

	ACE2	**TMPRSS2**	**furin**	**CD147**	**NRP-1**	**CD169**	**CD209**	**CD299**	**ASGR1**
Sinonasal tract									
CD169 *epithelial*					$\rho=0.554$ $p<0.001$				$\rho=0.502$ $p<0.001$
CD209 *epithelial*				$\rho=-0.425$ $p=0.005$					
CD299 *epithelial*					$\rho=0.542$ $p<0.001$				
KREMEN1 *epithelial*	$\rho=0.403$ $p=0.003$								
Conjunctivae									
CD169 *epithelial*			$\rho=0.515$ $p<0.001$						
CD169 *stromal*					$\rho=0.409$ (stromal) $p<0.001$			$\rho=0.763$ (stromal) $p<0.001$	
ASGR1 *epithelial*		$\rho=0.4$ $p=0.005$							
Bronchioli									

CD169		ρ=0.519 p<0.001	ρ=0.589 p<0.001	ρ=0.544 p<0.001	ρ=0.519 p<0.001			ρ=0.500 p<0.001	
ASGR1		ρ=0.491 p=0.001		ρ=0.406 p=0.003					

Table 3 Expression of ACE2, TMPRSS2, furin, CD147, NRP-1, CD169, CD209, CD299, ASGR1 and KREMEN1 in AMs. The following scores were applied: 0; no expression / negative; 1, low expression; 2, moderate expression; 3, high expression. Data for ACE2, TMPRSS2, furin and CD147 were obtained by reanalyzing TMAs from (43).

	Median	**Mean**	**negative, n/n (%)**	**low, n/n (%)**	**moderate, n/n (%)**	**high, n/n (%)**
ACE2	0	0.6	56/93 (60.2)	22/93 (23.7)	10/93 (10.8)	5/93 (5.4)
TMPRSS2	1	1.3	19/93 (20.4)	41/93 (44.1)	19/93 (20.4)	14/93 (15.1)
furin	2	2.2	3/93 (3.2)	19/93 (20.4)	28/93 (30.1)	43/93 (53.8)
CD147	2	2.2	4/93 (4.3)	18/93 (19.4)	30/93 (32.3)	41/93 (44.1)
NRP-1	1	0.9	41/92 (44.6)	28/92 (30.4)	16/92 (17.4)	7/92 (7.6)
CD169	1	1.3	14/92 (15.2)	46/92 (50.0)	22/92 (23.9)	10/92 (10.9)
CD209	0	0.7	50/91 (54.9)	25/91 (27.5)	11/91 (12.1)	5/91 (5.5)
CD299	0	0.7	52/92 (56.5)	18/92 (19.6)	16/92 (17.4)	6/92 (6.5)
ASGR1	1	1.0	38/92 (41.3)	26/92 (28.3)	16/92 (17.4)	12/92 (13.0)
KREMEN1	1	1.2	27/91 (29.7)	30/91 (33.0)	27/91 (29.7)	7/91 (7.7)

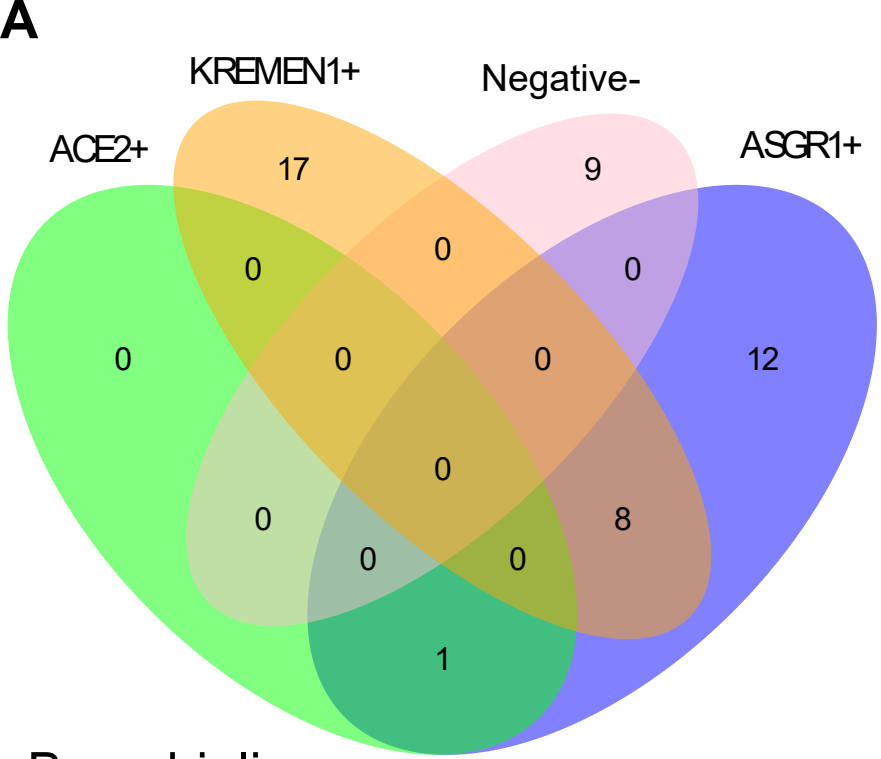
A
KREMEN1+
Negative-
ACE2+
ASGR1+
17
9
0
0
0
0
0
0
12
0
0
0
8
0
0
1
Bronchioli

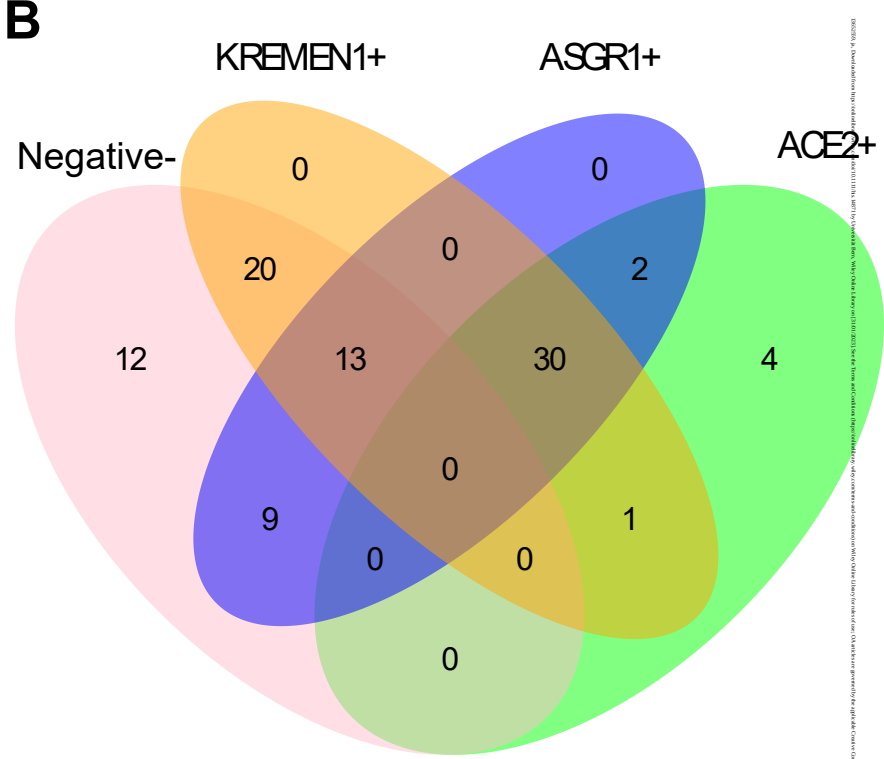
B
KREMEN1+
ASGR1+
Negative-
ACE2+
0
0
20
0
2
12
13
30
4
0
9
1
0
0
0
Alveolar macrophages